J Inorg Organomet Polym (2013) 23:976–981
DOI 10.1007/s10904-013-9880-3

Self-Assembled Organic–Inorganic Hybrid Nanocomposite of a Porphyrin Derivative and CdS

Peihua Zhu · Lingling Kan · Xingkui Guo · Xuewei Chen · Mingliang Ren · Yanli Chen · Xiaomei Zhang

Received: 15 February 2013 / Accepted: 14 May 2013 / Published online: 28 May 2013

Abstract A porphyrin derivative, 5-(4-carboxylphenyl)-10,15,20-tris(4-chlorophenyl) porphyrin (PorCOOH), was synthesized and self-assembled as a monolayer thin solid film on the modified surface of a quartz substrate by an ester bond between –COOH groups of PorCOOH molecules and –OH groups of the hydrophilic pretreated SiO_2 surface. An analysis of the spectral change revealed the *J*-aggregate nature of PorCOOH molecules in the obtained thin solid film. With this thin solid film of PorCOOH as a template, CdS nanoparticles were deposited on it in situ, which were further characterized by electronic absorption, fluorescence, and energy-dispersive X-ray spectroscopy. The morphology of CdS nanoparticles is disklike, and the diameter is ca. 40–60 nm, determined by scanning electronic microscopy. Furthermore, electron transfer between the organic layer and CdS nanoparticles was deduced through fluorescence quenching and theoretical analysis.

Keywords Porphyrin · CdS · Self-assembly · Organic–inorganic hybrid

1 Introduction

Organic–inorganic nanocomposite materials have been extensively studied over the past century due to their desirable optical, electrical, and magnetic properties. The combined unique properties offered by both organic–inorganic components on a nanoscale level make such nanocomposites attractive for a wide range of applications including next-generation optics, optoelectronic nanodevices, thin-film field-effect transistors, chemical or biological sensors, and catalysts with desirable optical, electrical, and magnetic properties [1–8]. There have also been many reports on the hybrid films of organic–inorganic nanoparticles of CdSe [5, 6], CdS [7, 8], TiO_2 [9, 10], Au [11], ZrO_2 [12], and MoS_2 [13], in which the organic–inorganic components interact through hydrogen bonding, van der Waals contacts, or electrostatic forces.

Self-assembly of functional molecular materials with large conjugated electronic structures into well-defined solid films depending on various non-covalent interactions including hydrogen bonding, amphiphilic effects, polar ability, electro-static interaction, ionic bonding, metal coordination, van der Waals forces, and π–π stacking has increasingly stimulated research interests in both the materials and chemistry fields [14–17]. As the one of the most important π conjugated systems, porphyrins have received extensive research interest due to their wide range of biologically relevant and industrial applications. For example, monomer, trimer, tetramer and extended wirelike nanostructures were produced by a cyano-substituted porphyrin on a gold surface [18]. Recently, the successful tuning control over the morphology of self-assembled nanostructures of porphyrin derivatives has been achieved by means of molecular design and synthesis through the introduction of metal–ligand coordination or hydrogen-bonding interactions [19–22].

In this paper, we describe the fabrication of an organic–inorganic hybride thin film composed of porphyrin and CdS, which involves the covalent immobilization of

The submission is intended for the 2nd International Congress on Advanced Materials.

P. Zhu (✉) · L. Kan · X. Guo · X. Chen · M. Ren · Y. Chen · X. Zhang
Key Laboratory of Chemical Sensing and Analysis in Universities of Shandong, School of Chemistry and Chemical Engineering, University of Jinan, Jinan 250022, China
e-mail: chm_zhuph@ujn.edu.cn

5-(4-carboxylphenyl)-10,15,20-tris(4-chlorophenyl) porphyrin (PorCOOH, Fig. 1) on a quartz surface and the in situ deposition of CdS nanoparticles on the thin solid film of surface-bound PorCOOH. The PorCOOH monolayers and CdS/PorCOOH hybrid films have been characterized by electronic absorption and fluorescence spectra, scanning electronic microscopy (SEM), and energy-dispersive X-ray spectroscopy (EDS). Significant fluorescent quenching can be detected in this hybrid system, indicating the presence of a strong interaction between the organic layer and inorganic nanoparticles. This research provided a new way to preparing given organic–inorganic nanostructures with a controlled molecular packing mode, which might find potential applications in optoelectronic devices.

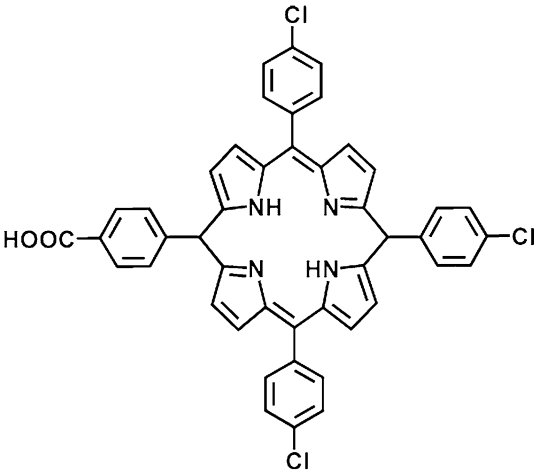

Fig. 1 Molecular structure of COOH–Por

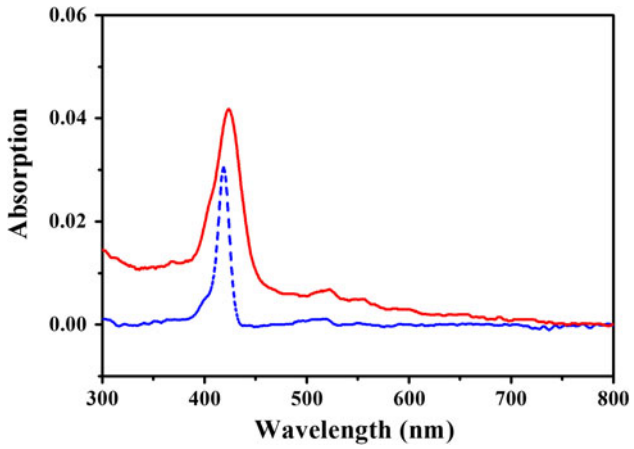

Fig. 2 Electronic absorption of PorCOOH in solution (*blue line*) and PorCOOH SA film (*red line*) (Color figure online)

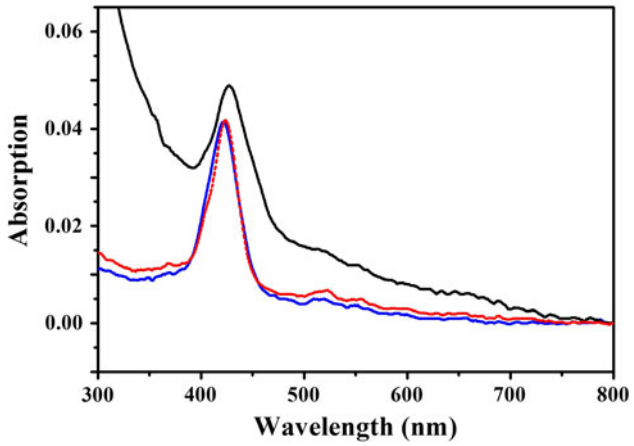

Fig. 3 Electronic absorption of PorCOOH SA film (*red line*), $CdCl_2$/PorCOOH SA film (*black line*) and CdS/PorCOOH SA film (*blue line*) (Color figure online)

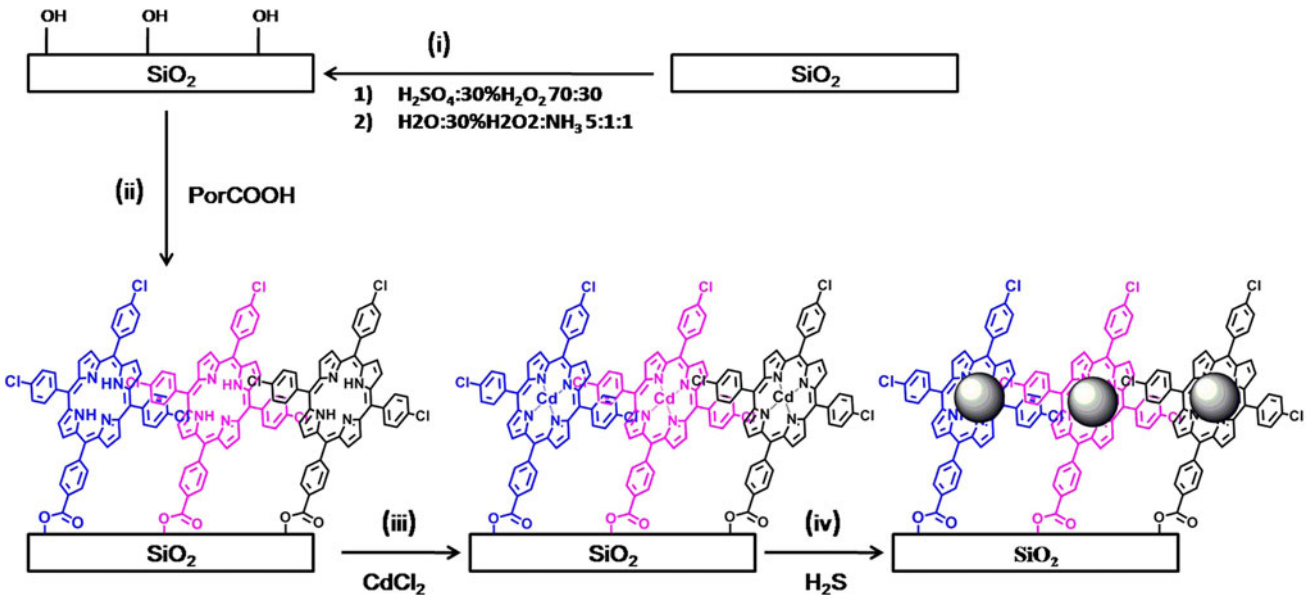

Scheme 1 Procedures for the Fabrication of the Hybrid CdS/PorCOOH SA Film (Color figure online)

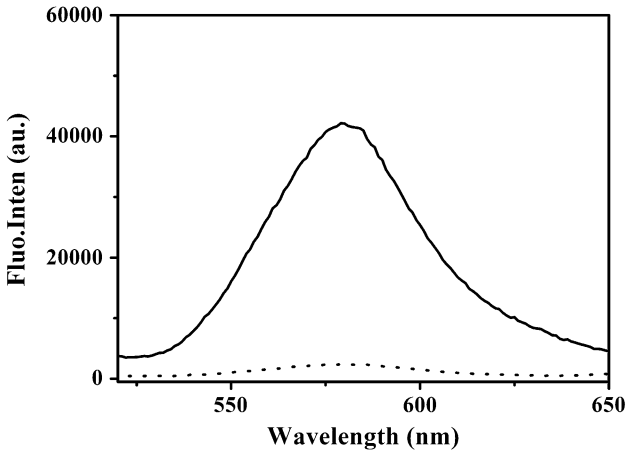

Fig. 4 Fluorescence emission spectra of the PorCOOH SA film (*solid line*) and the CdS/PorCOOH SA film (*dashed line*) at $\lambda_{ex} = 435$ nm

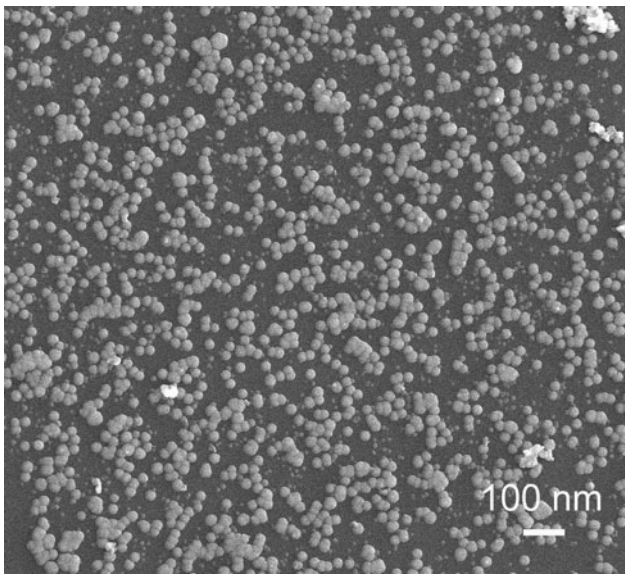

Fig. 5 EDS of the CdS nanoparticles deposited on the PorCOOH SA film

2 Experimental Section

2.1 Reagents and Apparatus

5-(4-Carboxylphenyl)-10,15,20-tris(4-chlorophenyl) porphyrin (PorCOOH) was synthesized and purified according to published procedures [23]. Dicyclohexyl carbodimide (DCC) was purchased from Aldrich. Dichloromethane for the preparation of self-assembled (SA) films of PorCOOH was freshly distilled from CaH_2 under nitrogen. Other reagents are used as received without further purification unless there is specific notation. Electronic absorption spectra were recorded on a Hitachi U-4100 spectro-photometer. The fluorescence spectra were measured on an

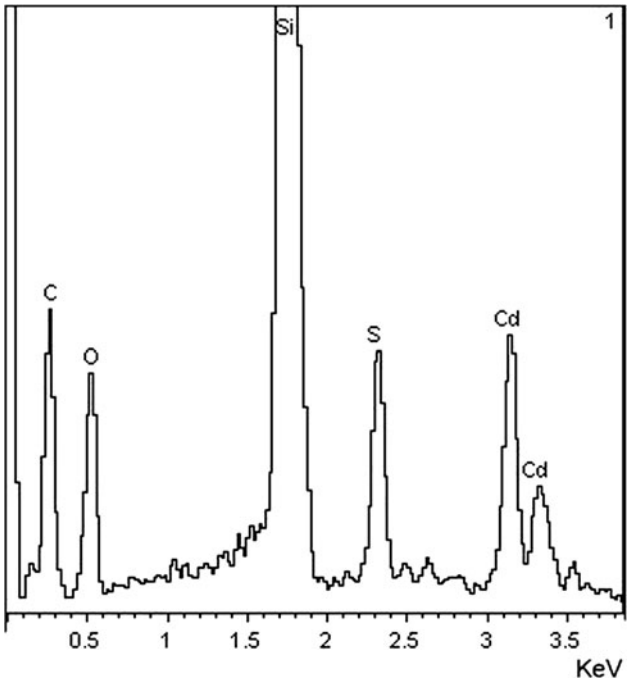

Fig. 6 EDS of the CdS nanoparticles deposited on the PorCOOH SA film

ISIS K2 system. Chemical compositions of the organic–inorganic hybrid nanocomposite were studied by energy-dispersive spectrometry (EDS) with an Oxford INCA X-sight instrument. Electrochemical measurements for PorCOOH solution were carried out with a BAS CV-50W voltammetric analyzer.

2.2 Preparation of the PorCOOH SA Film

A mixture of PorCOOH (24 mg, 0.0078 mmol) and DCC (1.6 mg, 0.0078 mmol) was dissolved in 20 mL of dichloromethane (solution 1). The preparation of the thin film required a two-step procedure (Scheme 1): (i) Quartz substrates were hydrophilically pretreated according to the published procedures. Substrates were first cleaned with piranha solution (7:3 v:v of 98 % H_2SO_4/30 % H_2O_2) at 80 °C for 1 h. Caution! Piranha solution is an extremely strong oxidizing reagent. Then they were repeatedly rinsed with doubly distilled water and immersed in an H_2O/30 % H_2O_2/NH_3 5:1:1 v/v/v mixture at room temperature for 40 min, washed again with doubly distilled water, and dried under vacuum just before the deposition of the coupling reagent. (ii) The newly treated quartz substrates were immersed in solution 1 for 24 h to bond PorCOOH molecules. Finally, the substrates bearing the covalently bonded PorCOOH molecules were repeatedly washed with dichloromethane to remove any residual unreacted PorCOOH, which resulted in a self-assembly film of PorCOOH (template 1).

2.3 Preparation of CdS Nanoparticles on the Modified PorCOOH SA Film

Template 1 was dipped into a $CdCl_2$ aqueous solution (0.14 mmol/L) for 12 h. After being washed with water, the thin film was subjected to drying in air. The dried film was placed in an atmosphere of H_2S gas liberated from a thioacet-amide aqueous solution at reduced pressure (Scheme 1).

3 Results and Discussion

3.1 Molecular Design

To connect porphyrin to the surface of SiO_2 covalently, a novel porphyrin derivative, namely, 5-(4-carboxylphenyl)-10,15,20-tris(4-chlorophenyl) porphyrin (PorCOOH, Fig. 1) was designed and prepared. Porphyrin rings are normally good electron acceptors/donor in most of the electron donor–acceptor pairs. Meanwhile, the carboxy phenyl unit linked at the meso positions of porphyrin ring provides sufficient flexibility for the optimization of both reactions of PorCOOH with hydrophilic pretreated SiO_2 surface and the noncovalent stacking of the porphyrin π systems.

3.2 Electronic Absorption Spectra

The electronic absorption of PorCOOH in CH_2Cl_2 is recorded in Fig. 2. As shown in Fig. 2, PorCOOH showed typical features of metal-free porphyrin compound, revealing the nonaggregated nature of both in dichloromethane. The strong absorption peak with a maximum at 419 nm and two weak absorption peaks with maxima at 520 and 550 nm for PorCOOH can be attributed to the porphyrin Soret band and Q bands, respectively. Compared to that of dichloromethane solution, all the Soret and Q absorption bands of the PorCOOH SA film showed red-shift from 419, 520 and 550 nm to 423, 522 and 556 nm. The changes in the electronic transitions are indicative of intermolecular dipole–dipole interaction between the porphyrin rings and thus the aggregation of the molecules. Kasha's point-dipole model provides a rationale for the observed band shifts and the split. The extreme case is represented by a head-to-tail arrangement of the dipoles, which results in a red-shifted band (*J* aggregate), and a blue-shifted band arises from a parallel arrangement of the dipoles (*H* aggregate) [24]. The red-shifted band components observed in the absorption spectrum of the SA film represent an intermediate case that results in apparent band splitting and is conventionally thought of as a slipped cofacial stack with an "edge-on" configuration on the surface of the substrate [25–27]. Compared to that in solution, the half bandwidth of the absorption bands of PorCOOH SA film increased (Fig. 2), indicating a slipped cofacial arrangement between adjacent porphyrin chromophores of the PorCOOH molecules (Scheme 1). This phenomenon has also been observed previously for the perylen aggregates with a slipped cofacial oriented structure, where two transition moments interact in face-to-face and parallel orientation to give rise to blue and red shifts respectively [27, 28].

With the above PorCOOH SA film as a template, the CdS nanoparticles were deposited. The electronic absorption spectra of the CdS/PorCOOH SA film and $CdCl_2$/PorCOOH SA film are also given in Fig. 3. For $CdCl_2$/PorCOOH SA film, the porphyrin Soret band at 423 nm are red shifted to 427 nm, indicating the formation of a Cd–N coordination bond between the nitrogen atoms of PorCOOH with the cadmium ion. As shown in Fig. 3, the higher absorption intensity at 422 nm of CdS/PorCOOH SA film is very similar to the absorption of PorCOOH SA film, which revealed the formation of CdS nanoparticle deposition.

3.3 Fluorescence Spectra

The fluorescence spectra of the PorCOOH SA film before and after CdS nanoparticle deposition at the same excitation wavelength ($\lambda_{ex} = 435$ nm) are shown in Fig. 4. It has been found that the emission spectra do not change much in shape after CdS deposition but the intensity decreases remarkably. This indicates that the fluorescence of the PorCOOH SA film has been quenched after CdS nanoparticle deposition. The fluorescence quenching efficiency is calculated to be as high as 97 %. The efficient fluorescence quenching might be induced by charge transfer or

Table 1 Half-wave redox potentials of PorCOOH (V vs SCE) in CH_2Cl_2 containing 0.1 M TBAP and the HOMO, LUMO levels of PorCOOH

Compound	Oxd_2 (V)	Oxd_1 (V)	Red_1 (V)	Red_2 (V)	E_{HOMO} (eV)[a]	E_{LUMO} (eV)[b]	$\Delta E^o_{1/2}$ (V)[c]
PorCOOH	1.65	1.36	−0.76	−1.21	−5.80	−3.68	2.12

[a] Calculated from empirical formula: HOMO = −(Oxd1 + 4.44 eV)

[b] LUMO = −(Red1 + 4.44 eV)

[c] ΔE^o is the potential difference between the first oxidation and first reduction processes, i.e. the HOMO–LUMO gap of corresponding molecule

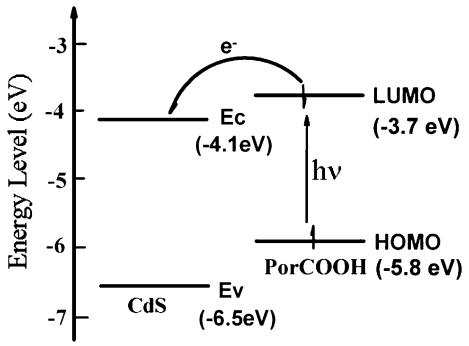

Scheme 2 Electron-Transfer Mechanism between PorCOOH and CdS Nanoparticles

energy transfer between the PorCOOH molecules and CdS nanoparticles. There is no overlap between the emission band of PorCOOH and the absorption band of CdS. Therefore, the energy transfer from PorCOOH to CdS nanoparticles is theoretically impossible. According to multiple reports in the literature, the photoinduced electron transfer between CdS and organic dyes dominates the fluorescence quenching process [5, 29, 30]. It is reasonable to assume that the fluorescence quenching in the present system proceeds by electron transfer between CdS and PorCOOH.

3.4 Morphology of the Aggregates

The SEM images were also captured after CdS deposition (Fig. 5). The morphology of the hybrid thin solid film is quite different from that of the PorCOOH SA film. It can be seen directly that CdS nanoparticles are grown on the surface of the PorCOOH SA film with mono disperse dimensions (Fig. 5). The average grain diameter is around 40–60 nm, which can be rationalized in terms of the period of the organic domains. The fact of preparing PorCOOH SA films modified by CdS nanoparticles was further validated by the elemental signatures of C, O, N, S, and Cd in the EDS as shown in Fig. 6. The atomic ratio of 1:1 for Cd versus S is indicative of the composite of the CdS nanoparticles.

3.5 Electrochemical Properties

The electrochemical properties of PorCOOH were studied by cyclic voltammetry (CV) in CH_2Cl_2, Table 1. The HOMO and LUMO levels have been evaluated using the half-wave redox potential values. The HOMO and LUMO energy values for PorCOOH are −5.8 and −3.7 eV with respect to the zero-vacuum level respectively, which can be inferred experimentally from the first one-electron oxidation and reduction process obtained for the electrochemical result [31]. However, the band gap of bulk cubic CdS is 2.4 eV with the conduction band (E_c) and valence band (E_v) at −4.1 and −6.5 eV with respect to the vacuum energy level. As the previous reports, these bulk material values are applicable to explaining the properties of small particles [32]. When PorCOOH molecules are excited, electrons of PorCOOH can be excited from the HOMO to the LUMO. The electron at the LUMO energy level of PorCOOH can easily transfer to the conducting band (E_c) of CdS (Scheme 2). The energy levels of PorCOOH (HOMO and LUMO)and CdS (E_v and E_c) are compatible for electron transfer with the PorCOOH molecule as the donor and the CdS nanoparticle as the acceptor.

4 Conclusion

In summary, CdS/PorCOOH hybrid films have been successfully prepared. There exists a strong interaction between the CdS nanostructure and PorCOOH molecules. Electron transfer may take place with PorCOOH as the donor and CdS as the acceptor. This kind of composite film with an organic–inorganic hybrid structure should have potential applications in a photoelectric conversion system. It is believed to be helpful in opening new possibilities for the construction of molecularly based nano-optoelectronics.

Acknowledgments Financial support from the Natural Science Foundation of China (Grant No. 21201079), the Education Department of Shandong province (Grant No. J12LD08), and the University of Jinan is gratefully acknowledged.

References

1. W. Bi, N. Louvain, N. Mercier, J. Luc, I. Rau, F. Kajzar, B. Sahraoui, Adv. Mater. **20**, 1013 (2008)
2. A. Kira, T. Umeyama, Y. Matano, K. Yoshida, S. Isoda, M. Isosomppi, N.V. Tkachenko, H. Lemmetyinen, H. Imahori, Langmuir **22**, 5497 (2006)
3. C.R. Kagan, D.B. Mitzi, C.D. Dimitrakopoulos, Science **286**, 945 (1999)
4. A. Nishimura, N. Sagawa, T.J. Uchino, Phys. Chem. C **113**, 4260 (2009)
5. L. Hu, Y.-L. Zhao, K. Ryu, C. Zhou, J.F. Stoddart, G. Grcuner, Adv. Mater. **20**, 939 (2008)
6. E. Hao, L. Wang, J. Zhang, B. Yang, X. Zhang, J. Shen, Chem. Lett. **1**, 5 (1999)
7. L. Sheeney-Haj-Ichia, B. Basnar, I. Willner, Angew. Chem. Int. Ed. **44**, 78 (2005)
8. N.A. Kotov, I. Dekany, J.H. Fendler, J. Phys. Chem. **99**, 13065 (1995)
9. K. Tadanaga, J. Morinaga, A. Matsuda, T. Minami, Chem. Mater. **12**, 590 (2000)
10. J.F. Liu, K.Z. Yang, Z.H. Lu, J. Am. Chem. Soc. **119**, 11061 (1997)
11. T. Cassagneau, J.H. Fendler, T.E. Mallouk, Langmuir **16**, 241 (2000)

12. E.-H. Kang, P. Jin, Y. Yang, J. Sun, J. Shen, Chem. Commun. **41**, 4332 (2006)
13. H. Tachibana, Y. Yamanaka, H. Sakai, M. Abe, M. Matsumoto, Chem. Mater. **12**, 854 (2000)
14. J.A.A. Elemans, W.R. Hameren, R.J.M. Nolte, A.E. Rowan, Adv. Mater. **18**, 1251 (2006)
15. G. Lu, Y. Chen, Y. Zhang, M. Bao, Y. Bian, X. Li, J. Jiang, J. Am. Chem. Soc. **130**, 11623 (2008)
16. S. Cui, H. Liu, L. Gan, Y. Li, D. Zhu, Adv. Mater. **20**, 2918 (2008)
17. C. Huang, Y. Li, Y. Song, Y. Li, H. Liu, D. Zhu, Adv. Mater. **22**, 3532 (2010)
18. T. Yokoyama, S. Yokoyama, T. Kamikado, Y. Yoshi-shige Okuno, T. Mashiko, Nature **413**, 619 (2001)
19. Y. Gao, X. Zhang, C. Ma, X. Li, J. Jiang, J. Am. Chem. Soc. **130**, 17044 (2008)
20. Y. Gao, Y. Chen, R. Li, Y. Bian, X. Li, J. Jiang, Chem. Eur. J. **15**, 13241 (2009)
21. G. Lu, Y. Chen, Y. Zhang, M. Bao, Y. Bian, X. Li, J. Jiang, J. Am. Chem. Soc. **130**, 11623 (2008)
22. G. Lu, X. Zhang, X. Cai, J. Jiang, Eur. J. Inorg. Chem. **10**, 753 (2010)
23. P. Bhyrappa, C. Arunkumar, J.J. Vittal, J. Chem. Sci. **117**, 139 (2005)
24. M. Kasha, H.R. Rawls, M.A. El-bayoumi, Pure Appl. Chem. **11**, 371 (1965)
25. V. Czikklely, H.D. Forsterling, H. Kuhn, Chem. Phys. Lett. **6**, 207 (1970)
26. N. Nagata, S. Kugimiya, Y. Kobuke, Chem. Commun. **28**, 1389–1390 (2000)
27. I.K. Iverson, S.M. Casey, W. Seo, S.-W. Tam-Chang, B.A. Pindzola, Langmuir **18**, 3510 (2002)
28. Y. Kobuke, H. Miyaji, J. Am. Chem. Soc. **116**, 4111 (1994)
29. R. Schroeder, B. Ullrich, Appl. Phys. Lett. **81**, 556 (2002)
30. A. Boulesbaa, A. Issac, D. Stockwell, Z. Huang, J. Huang, J. Guo, T. Lian, J. Am. Chem. Soc. **129**, 15132 (2007)
31. S. Vajiravelu, L. Ramunas, G.J. Vidas, G. Valentas, J. Vygintas, S. Valiyaveettil, J. Mater. Chem. **19**, 4268 (2009)
32. A. Hasselbarth, A. Eychmiiller, H. Weller, Chem. Phys. Lett. **203**, 271 (1993)